Steel and Composite Structures, *Vol. 19, No. 2 (2015) 327-348*
DOI: http://dx.doi.org/10.12989/scs.2015.19.2.327

Dimensionless analysis of composite rectangular and circular RC columns

Ali Massumi * and Alireza Badkoubeh [a]

Department of Civil Engineering, Faculty of Engineering, Kharazmi University, No. 43, Dr. Mofatteh Ave., Tehran 15719-14911, Iran

(*Received April 15, 2014, Revised December 23, 2014, Accepted January 09, 2015*)

Abstract. A numerical procedure is presented that provides ultimate curvature and moment domains for composite rectangular and circular cross-sections of reinforced concrete columns with or without an embedded steel section subjected to combined axial loading and biaxial bending. The stress resultants for the concrete and reinforcement bars are calculated using fiber analysis and the stress resultants for the encased structural steel are evaluated using an exact integration of the stress-strain curve over the area of the steel section. A dimensionless formula is proposed that can be used for any section with similar normalized geometric and mechanical parameters. The contribution of each material to the bearing capacity of a section (resistance load and moments) is calculated separately so that the influence of each geometric or mechanical parameter on the bearing capacity can be investigated separately.

Keywords: biaxial bending; composite columns; dimensionless formulation; rectangular and circular cross-sections; ultimate strength analysis

1. Introduction

In framed composite or reinforced-concrete (RC) structures where columns are subjected to biaxial eccentric loading, the ultimate bearing capacity of the cross-sections is critical to the total strength of the structure. Technical codes (Eurocode 2 2005, ACI 318 2008) are useful for the analysis and design of common RC rectangular and circular members with symmetric distributions of longitudinal reinforcement because they assume that the bending moment components act separately along the principal axes. Simplifying the assumptions used in technical codes for stress-strain diagrams of materials can reduce the accuracy of the analysis. To achieve a precise analysis expressing the real state of stress, both axial loading and biaxial bending must be considered.

Numerous methods have been proposed to reduce these deficiencies and increase the accuracy of the analysis. Rotter (1985) presented an inelastic analysis of a composite section subjected to axial loading and biaxial bending based on Green's theorems. This method allowed for exact

*Corresponding author, Associate Professor, E-mail: massumi@khu.ac.ir
[a] M.Sc. in Structural Engineering, E-mail: ar.badkoubeh@gmail.com

http://www.techno-press.org/?journal=scs&subpage=8 ISSN: 1229-9367 (Print), 1598-6233 (Online)

determination of stress resultants where the stress-strain relation of the materials was integrable for a given set of deformations and the section boundary was rectilinear. Rodriguez and Aristizabal-Ochoa (1999) used the Gauss integral method for equilibrium, a nonlinear stress-strain relationship for concrete, and a multi-linear elastoplastic relationship for reinforcement bars to evaluate the theoretical ultimate strength of RC short columns subjected to axial loading and biaxial bending.

Chen *et al*. (2001) presented an iterative Quasi-Newton procedure based on the Regula-Falsi numerical scheme. They evaluated the stress resultants for concrete by integrating the concrete stress-strain curve over the compression zone and using the fiber element method for the stress resultants of the encased structural steel and reinforcement. The procedure provided an efficient and accurate analysis for short composite columns of arbitrary cross-sections.

Bonet *et al*. (2004) presented an integration procedure to analyze arbitrary RC sections subjected to axial forces and biaxial bending. The method was used for a general stress field for sections where the stress field was uniform in at least one direction. Bonet *et al*. (2006) also presented a comparative study to design RC sections under biaxial bending based on different integration methods for stress. A numerical procedure for analyzing composite and RC sections of arbitrary polygonal shapes was presented by Sousa and Muniz (2007). Their method applied an analytical integration of a cross section.

Charalampakis and Koumousis (2008) presented a method based on analytically basic surface integrals that provided the ultimate strength of arbitrary composite sections under axial loading and biaxial bending. In this method, the geometry of a cross-section was described by curvilinear trapezoids having straight or curved edges. Fossetti and Papia (2012) proposed a numerical procedure for analysis of RC rectangular sections with symmetrical longitudinal reinforcement bars subjected to axial loading and biaxial bending.

The present study proposes a new iterative procedure to analyze rectangular and circular cross-sections of steel-reinforced concrete composite columns under axial loading and biaxial bending. It uses a basic surface integral algorithm for encased structural steel and the fiber method for concrete and reinforcements. The sections are symmetric with respect to the principal axes and the ultimate curvature and moment domains are obtained. A dimensionless formula is adopted for sections having the same normalized geometric and mechanical parameters where one analysis result can be used. This simplifies and decreases the computational cost over dimensional values.

2. Section geometry and reinforcement arrangement of rectangular section

The expressions and the procedure presented in the following section and proposed in the limit state of rectangular section and the material constitutive laws of concrete and reinforcement are those expressed by Fossetti and Papia (2012) which are used in this study.

The x, y Cartesian system is the orientation of the principal axes at the centroid of a section. The rectangular section under study has a width b and height h. The distribution of the longitudinal reinforcement bars is symmetric with respect to the principal axes and consisted of (Fig. 1):

- 4 bars of equal diameter at each corner of the section having a total area A_{rc},
- n_b bars of equal diameter at the top and bottom of the section parallel to b and between the corner bars having a total area A_{rb}, and
- n_h bars of equal diameter at the left and right sides of the section parallel to h and between the corner bars having a total area A_{rh}.

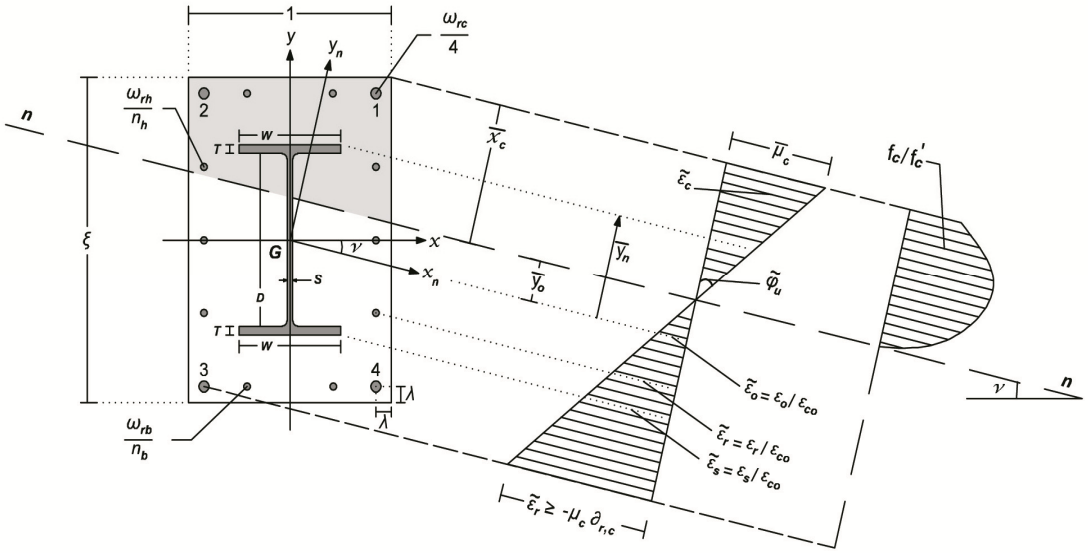

Fig. 1 Ultimate state of composite rectangular section under axial loading and biaxial bending

The dimensionless parameters for the distribution of reinforcement are

$$\omega_{rc} = \frac{A_{rc}}{bh}\frac{f_{yr}}{f_c'} \quad \omega_{rb} = \frac{A_{rb}}{bh}\frac{f_{yr}}{f_c'} \quad \omega_{rh} = \frac{A_{rh}}{bh}\frac{f_{yr}}{f_c'} \tag{1}$$

where f_{yr} is the yielding stress of the reinforcement bars, f'_c is the cylindrical strength of the concrete and $b \times h$ is the area of the concrete core. The reinforcement ratio for the section (ACI 318 2008, Eurocode 2 2005) is expressed as

$$\rho_r = \left[\omega_{rc} + 2(\omega_{rb} + \omega_{rh})\frac{f_c'}{f_{yr}} \right] \tag{2}$$

The distance between the centroid of the reinforcement bars and the closest section surface in directions b and h is denoted by c. The dimensionless parameters denoting the section geometry are the ratios

$$\lambda = \frac{c}{b} \qquad \xi = \frac{h}{b} \tag{3}$$

and for the steel section are

$$W = \frac{b_f}{b} \qquad D = \frac{h_w}{b} \qquad T = \frac{t_f}{b} \qquad S = \frac{t_w}{b} \tag{4}$$

where b_f is the flange width, h_w is the web height, t_f is the flange thickness, and t_w is the web thickness of the structural steel as shown in Fig. 1.

3. Limit state of rectangular section

The basic assumptions used in this method are:

- Concrete tensile strength is neglected and plane sections remain planar (strain compatibility)
- Limit state of the section is assumed and the outermost concrete compression fiber equals the ultimate strain of the concrete at the end of the post-peak branch describing the softening behavior (ε_{cu})

Fig. 1 shows a limit state for a rectangular section under axial loading and biaxial bending. The location of the neutral axis is determined by angle v and distance x_c (the distance from the neutral axis to the point of maximum shortening strain). Dividing x_c by b provides the dimensionless value

$$\bar{x}_c = \frac{x_c}{b} \tag{5}$$

Other section dimensions are normalized with respect to b and all strains with respect to ε_{co} (concrete strain corresponding to f'_c). The normalized parameters are denoted by superscripts (−) for length and distance and (~) for strain and curvature.

The normalized center-to-center distance of the reinforcing bars in directions b and h are

$$\bar{L}_b = \frac{1-2\lambda}{n_b+1} \qquad \bar{L}_h = \frac{\xi-2\lambda}{n_h+1} \tag{6}$$

φ_u is a curvature normalized with respect to ε_{co} as

$$\tilde{\varphi}_u = \frac{\varphi_u b}{\varepsilon_{co}} = \frac{\varepsilon_{cu}}{\varepsilon_{co}}\frac{b}{x_c} = \frac{\mu_c}{\bar{x}_c} \tag{7}$$

where

$$\mu_c = \frac{\varepsilon_{cu}}{\varepsilon_{co}} \tag{8}$$

ε_{cu} denotes the ultimate strain of the concrete. By considering N as the average compressive axial force, the normalized ratio is

$$n = \frac{N}{bhf'_c} \tag{9}$$

The resistance moment and domain of the ultimate curvature can be obtained in dimensionless form for any angle v within range $0 \le v \le \pi/2$. Thus, the normalized ultimate moments along the principal axes are

$$m_{ux} = \frac{M_{ux}}{b^2 hf'_c} \qquad m_{uy} = \frac{M_{uy}}{b^2 hf'_c} \tag{10}$$

and the dimensionless curvature components are

$$\tilde{\varphi}_{ux} = \tilde{\varphi}_u \cos v \qquad \tilde{\varphi}_{uy} = \tilde{\varphi}_u \sin v \tag{11}$$

4. Material constitutive laws

4.1 Confined concrete

The concrete strain at any point (ε_c) is normalized with respect to ε_{co}. Consequently, the dimensionless stress of concrete is defined as

$$\frac{f_c}{f'_c} = H(\widetilde{\varepsilon}_c) \qquad 0 \le \widetilde{\varepsilon}_c \le \mu_c \tag{12}$$

where H is a function of $\widetilde{\varepsilon}_c$. Eq. (12) can be expressed by one function (Sargin 1971, Mander *et al*. 1988) or two analytical expressions (Saatcioglu and Razvi 1992, Vallenas *et al*. 1997). One expression denotes the ascending branch from zero to f'_c ($0 \le \widetilde{\varepsilon}_c \le 1$) and the other denotes the post-peak branch ($1 \le \widetilde{\varepsilon}_c \le \mu_c$) in the stress-strain diagram of the concrete as shown in Fig. 2. Adopting analytical expressions (Saatcioglu *et al*. 1995, Campione *et al*. 2010) yields

$$H(\widetilde{\varepsilon}_c) = (2\widetilde{\varepsilon}_c - \widetilde{\varepsilon}_c^2)^{\alpha} \qquad 0 \le \widetilde{\varepsilon}_c \le 1 \tag{13a}$$

$$H(\widetilde{\varepsilon}_c) = 1 + \eta_c(\widetilde{\varepsilon}_c - 1) \qquad 0 \le \widetilde{\varepsilon}_c \le \mu_c \tag{13b}$$

where η_c is the softening modulus of post-peak branch normalized with f'_c / ε_{co} and α depends on the confinement effects. If the transverse reinforcement has a good effect on the confinement, α, η_c and μ_c can be considered to be 0.7, -0.1 and 3.0, respectively (Fossetti and Papia 2012). Otherwise, these values should be obtained analytically.

4.2 Steel reinforcement

The stress-strain relationship of reinforcement is considered to be linear up to the yielding point (f_{yr}) corresponding to ± ε_{yr}. After that, it is replaced up to rupture strain (± ε_{ur}) by a linear branch having a constant slope equal to the hardening modulus E_h, as shown in Fig. 3. Based on these assumptions, the dimensionless stress of reinforcement is

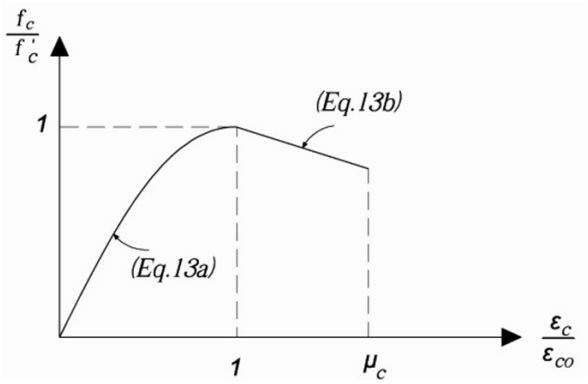

Fig. 2 The normalized stress-strain diagram of concrete

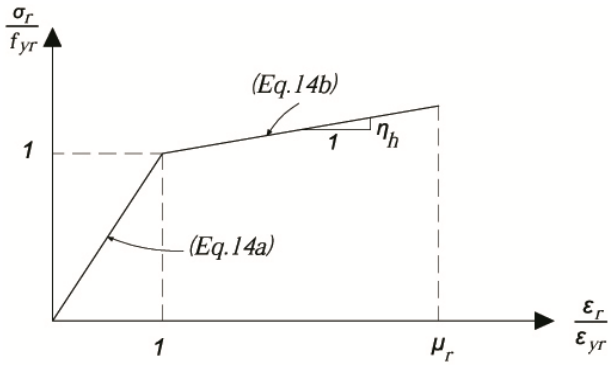

Fig. 3 The normalized stress-strain diagram of steel

$$\frac{\sigma_r}{f_{yr}} = \frac{\varepsilon_r}{\varepsilon_{yr}} \qquad \left|\frac{\varepsilon_r}{\varepsilon_{yr}}\right| \le 1 \tag{14a}$$

$$\frac{\sigma_r}{f_{yr}} = \sin n\left\{\frac{\varepsilon_r}{\varepsilon_{yr}}\right\}\left[1+\eta_h\left(\left|\frac{\varepsilon_r}{\varepsilon_{yr}}\right|-1\right)\right] \qquad 1 \le \left|\frac{\varepsilon_r}{\varepsilon_{yr}}\right| \le \mu_r \tag{14b}$$

where

$$\eta_h = \frac{E_h}{E_s} \qquad \mu_r = \frac{\varepsilon_{ur}}{\varepsilon_{yr}} \tag{15}$$

In Eq. (15), E_h is the average hardening modulus and E_s is the modulus of elasticity. In addition, Eq. (14b) can be expressed as an accurate expression (Chang and Mander 1994) instead of a bilinear relationship. Since all the strains are normalized with respect to ε_{co}, another expression is required to relate the characteristic strain values of concrete and reinforcement. The latter is defined by

$$\partial_{r,c} = \frac{\varepsilon_{yr}}{\varepsilon_{co}} \tag{16}$$

Note that the compressive stresses and shortening strains are considered to be positive values and tensile stresses and elongations are assumed to be negative for all materials.

4.3 Structural steel

The x_n axis is considered to be parallel to the neutral axis; therefore, the rotated $x_n y_n$ Cartesian system can be defined at the centroid of the section. All the coordinates in the xy Cartesian system can be expressed in the rotated $x_n y_n$ Cartesian system by the rotational transformation

$$\begin{bmatrix} x_n \\ y_n \end{bmatrix} = \begin{pmatrix} \cos v & -\sin v \\ \sin v & \cos v \end{pmatrix} \begin{bmatrix} x \\ y \end{bmatrix} \tag{17}$$

where angle v is assumed to be positive in the clockwise direction. The normalized strain at any point on a steel section can be expressed as a function of distance from the x_n axis

$$\widetilde{\varepsilon}_s(\bar{y}_n) = \widetilde{\varepsilon}_o + \widetilde{\varphi}_u.\bar{y}_n \tag{18}$$

where $\widetilde{\varepsilon}_o$ is the normalized strain at the origin and $\bar{y}_n$ is the normalized distance from the x_n axis. The value of $\widetilde{\varepsilon}_o$ is derived from Fig. 1 as

$$\widetilde{\varepsilon}_o = \frac{\mu_c}{\bar{x}_c} \cdot \bar{y}_o \tag{19}$$

where

$$\bar{y}_o = \bar{d}_{n,c,3} - \bar{d}_{x_n,c,3} \tag{20}$$

$\bar{d}_{n,c,3}$ and $\bar{d}_{x_n,c,3}$ are the normalized distances of corner bar 3 from the neutral and x_n axes, respectively. As shown in Eq. (17), the x, y coordinates can be transformed into x_n, y_n coordinates. This can be done for any value of v. It is assumed that any segment on the stress-strain diagram of steel is expressed by a cubic polynomial expression. Therefore, the normalized stress-strain relation at any point of the steel section is

$$\widetilde{\sigma}_s = \sum_{i=0}^{3} (a_i.\widetilde{\varepsilon}_s^{\,i}) \tag{21}$$

where the coefficient a_i is known from the properties of the steel and specified by arbitrary points on the stress-strain diagram. Substituting Eq. (18) into Eq. (21) obtains

$$\widetilde{\sigma}_s = \sum_{i=0}^{3} (b_i.\bar{y}_n^{\,i}) \tag{22}$$

where

$$\begin{aligned} b_o &= a_o + a_1.\widetilde{\varepsilon}_o + a_2.\widetilde{\varepsilon}_o^{\,2} + a_2.\widetilde{\varepsilon}_o^{\,3} \\ b_1 &= 3.a_3.\widetilde{\varepsilon}_o^{\,3}.\widetilde{\varphi}_u + 2.a_2.\widetilde{\varepsilon}_o.\widetilde{\varphi}_u + a_1.\widetilde{\varphi}_u \\ b_2 &= 3.a_3.\widetilde{\varepsilon}_o.\widetilde{\varphi}_u^{\,2} + a_2.\widetilde{\varphi}_u^{\,2} \\ b_3 &= a_2.\widetilde{\varphi}_u^{\,3} \end{aligned} \tag{23}$$

5. Contribution of materials to the bearing capacity of rectangular section

5.1 Contribution of concrete core

The compressed region in the concrete is divided into N_{st} strips parallel to the neutral axis. All the strips have the same normalized height

$$\bar{h} = \frac{\bar{x}_c}{N_{st}} \tag{24}$$

and are numbered from 1 to k with the first strip being the farthest fiber of the compressed concrete from the neutral axis. Fig. 4 shows the typical division and numbering of the strips. The concrete contribution to the stress is measured at mid-height of the strips at its centroid (G_k). The kth strip has the normalized length $\bar{l}_k$ and the normalized height is

$$\bar{e}_k = (k-0.5)\bar{h} \tag{25}$$

The area of each strip is $\bar{e}_k.\bar{h}$ normalized with respect to b^2. The normalized distances of the strips from the neutral axis are expressed by

$$\bar{d}_{n,k} = \bar{x}_c - \bar{e}_k = \bar{x}_c - (k-0.5)\bar{h} \tag{26}$$

These normalized distances are presented in Table 1 where $\bar{l}_v$ is equal to

$$\bar{l}_v = \sin v + \xi \cos v \tag{27}$$

Four cases are considered in Fig. 5:

- Case 1: Fig. 3(a) if $\bar{e}_k \le \sin v$ & $\bar{e}_k \le \xi \cos v$
- Case 2: Fig. 3(b) if $\bar{e}_k \ge \sin v$ & $\bar{e}_k \le \xi \cos v$
- Case 3: Fig. 3(c) if $\bar{e}_k \le \sin v$ & $\bar{e}_k \ge \xi \cos v$
- Case 4: Fig. 3(d) if $\bar{e}_k \ge \sin v$ & $\bar{e}_k \ge \xi \cos v$

The contribution of the concrete core to the strength of the section (the normalized axial load) and the ultimate moments along the x and y axes are

$$n_c = \frac{N_c}{bhf'_c} = \frac{\bar{h}}{\xi}\sum_{k=1}^{N_{st}} \bar{l}_k \frac{f_{c,k}}{f'_c} \tag{28a}$$

$$m_{uc,j} = \frac{M_{uc,j}}{b^2 h f'_c} = \frac{M_{uc,j}}{b^3 \xi} = \frac{\bar{h}}{\xi}\sum_{k=1}^{N_{st}} \bar{l}_k.\bar{d}_{j,k} \frac{f_{c,k}}{f'_c}; \qquad (j = x, y) \tag{28b}$$

The expression $f_{c,k}/f'_c$ in Eq. (28) is calculated using Eq. (12). The strain at any point on the concrete can be stated as

$$\tilde{\phi}_{c,k} = \bar{d}_{n,k}.\tilde{\varphi}_u \tag{29}$$

5.2 Contribution of reinforcement

The normalized distances of the reinforcement bars are defined by $\bar{d}_{a,t,k}$ where

- a: coordinate axes (n, x, y, x_n, y_n)
- t: type of reinforcement; corners (c), top of section in direction b (bu), bottom of section in direction b (bl), left side of section in direction h (hl), right side of section in direction h (hr)
- k: number of bars; 1, 2,…, 4 for corner bars, 1, 2,…, n_b for $t = bu$, and $t = bl$, 1, 2,…, n_h for $t = hr$ and $t = hl$

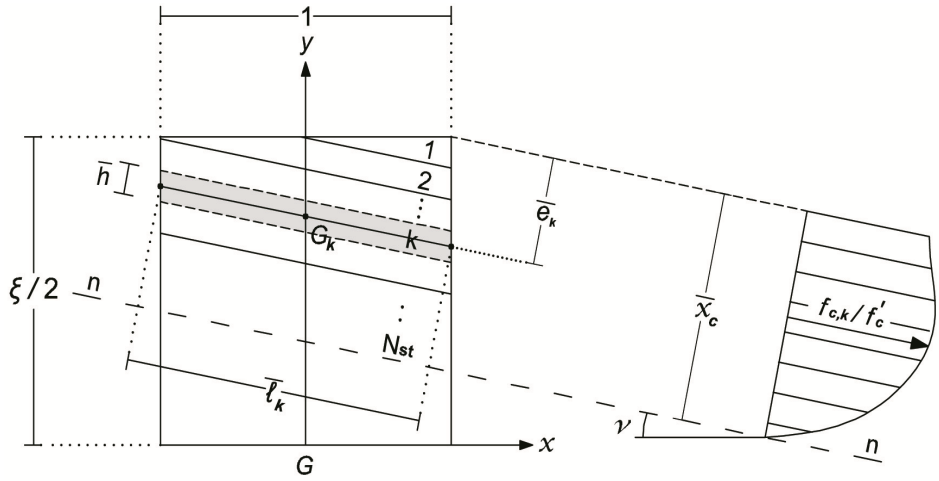

Fig. 4 Strip model of compressed concrete region in rectangular section

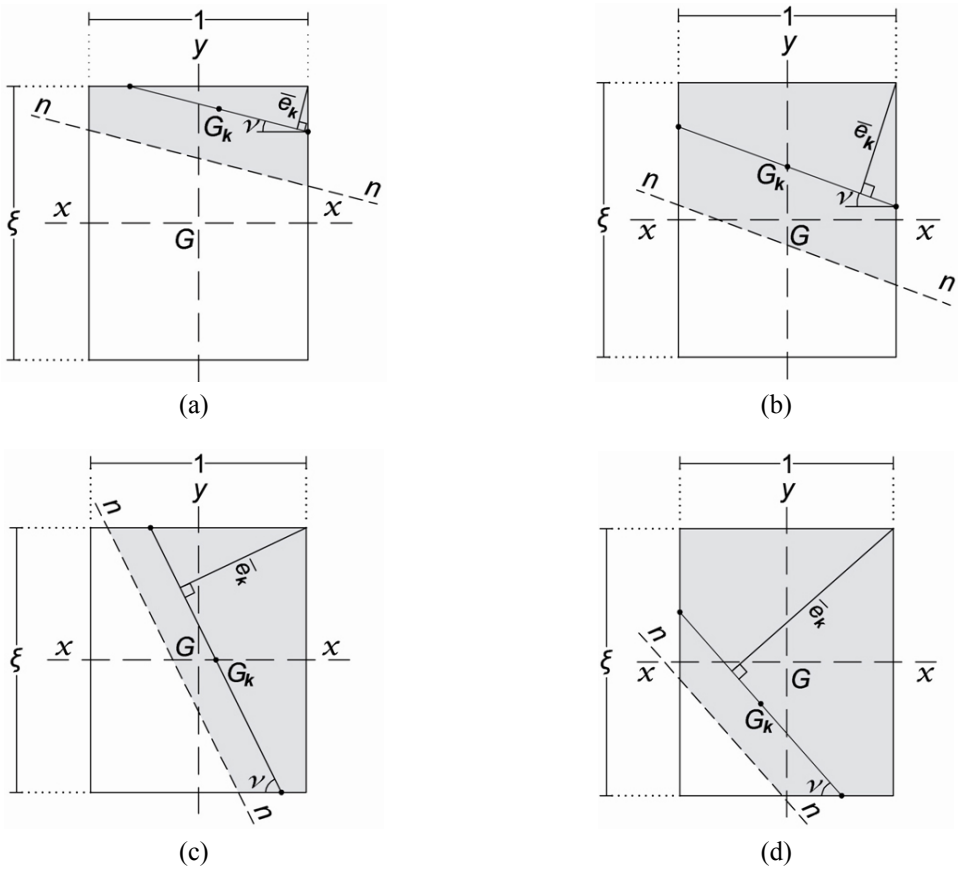

Fig. 5 Possible cases of position for mid-height segment of *k*th strip of compressed concrete in rectangular section

Table 1 Expressions of $\bar{l}_k$, $\bar{d}_{x,k}$ and $\bar{d}_{y,k}$ for kth strip in compressed concrete

case	$\bar{l}_k$	$\bar{d}_{x,k}$	$\bar{d}_{y,k}$
1	$2\bar{e}_k / \sin(2v)$	$0.5(\xi - \bar{l}_k \sin v)$	$0.5(\xi - \bar{l}_k \cos v)$
2	$1 / \cos v$	$0.5(\xi + \bar{l}_k \sin v) - \bar{e}_k / \cos v$	0
3	$\xi / \sin v$	0	$0.5(1 + \bar{l}_k \cos v) - \bar{e}_k / \sin v$
4	$2(\bar{l}_k - \bar{e}_k) / \sin(2v)$	$-0.5(\xi - \bar{l}_k \sin v)$	$-0.5(\xi - \bar{l}_k \cos v)$

The stress (σ_r) and strain (ε_r) of the kth bar for type t are denoted as $\sigma_{r,t,k}$ and $\varepsilon_{r,t,k}$, respectively. Fig. 6 shows the type and number of bars and Fig. 7 shows the normalized distances of the corner bars from the neutral axis. In Fig. 7, the latter is expressed as

$$\begin{aligned} \bar{d}_{n,c,1} &= \bar{x}_c - \lambda(\sin v + \cos v) & \bar{d}_{n,c,2} &= \bar{d}_{n,c,1} - (1-2\lambda)\sin v \\ \bar{d}_{n,c,3} &= \bar{d}_{n,c,2} - (\xi - 2\lambda)\cos v & \bar{d}_{n,c,4} &= \bar{d}_{n,c,1} - (\xi - 2\lambda)\cos v \end{aligned} \tag{30}$$

and the normalized distances of the corner bars from the x and y axes are

$$\begin{aligned} \bar{d}_{x,c,1} &= \bar{d}_{x,c,2} = 0.5(\xi - 2\lambda) & \bar{d}_{x,c,3} &= \bar{d}_{x,c,4} = -0.5(\xi - 2\lambda) \\ \bar{d}_{y,c,1} &= \bar{d}_{y,c,4} = 0.5(1-2\lambda) & \bar{d}_{y,c,2} &= \bar{d}_{y,c,3} = -0.5(1-2\lambda) \end{aligned} \tag{31}$$

Normalized distances for other types of reinforcement are shown in Table 2. For a specific value of angle v, if $\bar{x}_c$ is known, the dimensionless curvature can be obtained from Eq. (7) and the normalized strain of the kth bar of type t as

$$\frac{\varepsilon_{r,t,k}}{\varepsilon_{yr}} = \frac{\tilde{\varphi}_u}{\partial_{r,c}} \bar{d}_{n,t,k} \tag{32}$$

Then, $\sigma_{r,t,k}/f_{yr}$ can be calculated using Eq. (14). The contribution of reinforcement is

$$n_r = \frac{N_r}{bhf_c'} = \frac{\omega_{rc}}{4}\sum_{k=1}^{4}\frac{\sigma_{r,c,k}}{f_{yr}} + \frac{\omega_{rb}}{n_b}\sum_{k=1}^{n_b}\left(\frac{\sigma_{r,bu,k}}{f_{yr}} + \frac{\sigma_{r,bl,k}}{f_{yr}}\right) + \frac{\omega_{rh}}{n_h}\sum_{k=1}^{n_h}\left(\frac{\sigma_{r,hr,k}}{f_{yr}} + \frac{\sigma_{r,hl,k}}{f_{yr}}\right) \tag{33a}$$

$$\begin{aligned} m_{ur,j} = \frac{M_{ur,j}}{b^2 hf_c'} = \frac{M_{uc,j}}{b^3\xi} &= \frac{\omega_{rc}}{4}\sum_{k=1}^{4}\frac{\sigma_{r,c,k}}{f_{yr}}\bar{d}_{j,c,k} \\ &+ \frac{\omega_{rb}}{n_b}\sum_{k=1}^{n_b}\left(\frac{\sigma_{r,bu,k}}{f_{yr}}\bar{d}_{j,bu,k} + \frac{\sigma_{r,bl,k}}{f_{yr}}\bar{d}_{j,bl,k}\right) \qquad (j = x, y) \\ &+ \frac{\omega_{rh}}{n_h}\sum_{k=1}^{n_h}\left(\frac{\sigma_{r,hr,k}}{f_{yr}}\bar{d}_{j,hr,k} + \frac{\sigma_{r,hl,k}}{f_{yr}}\bar{d}_{j,hl,k}\right); \end{aligned} \tag{33b}$$

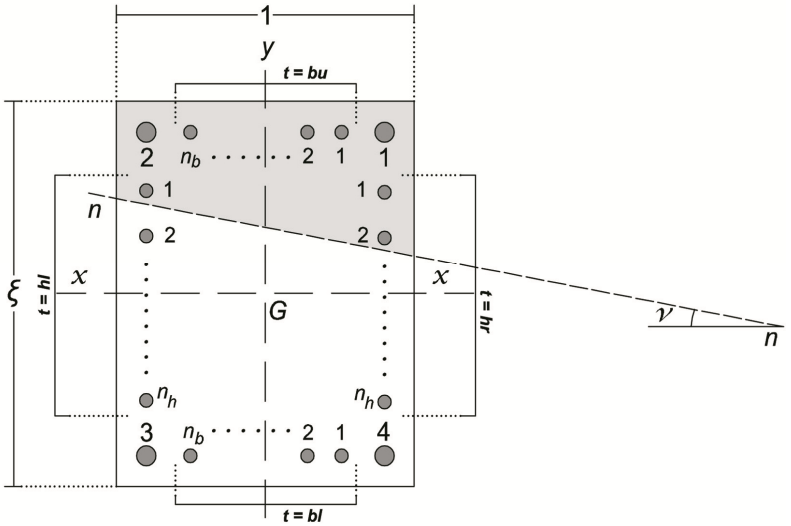

Fig. 6 Type and numbering of reinforcement bars in rectangular section

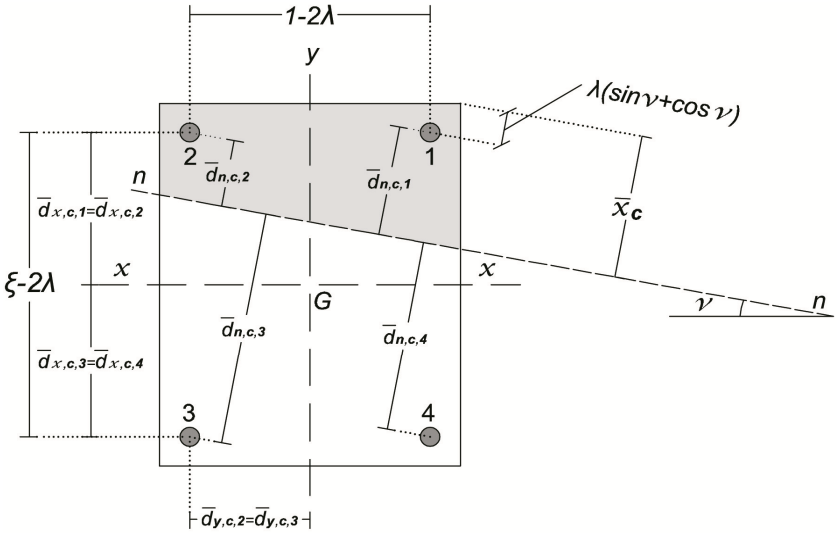

Fig. 7 Normalized distances of corner bars from the *n*, *x*, and *y* axes in rectangular section

Table 2 Normalized distances of *k*th bar for type *t* from the *n*, *x* and *y* axes

type	$\bar{d}_{n,t,k}$	$\bar{d}_{x,t,k}$	$\bar{d}_{y,t,k}$
$t = bu$	$\bar{d}_{n,c,1} - k\bar{L}_b \sin v$	$0.5(\xi - 2\lambda)$	$\bar{d}_{y,c,1} - k\bar{L}_b$
$t = bl$	$\bar{d}_{n,c,4} - k\bar{L}_b \sin v$	$-0.5(\xi - 2\lambda)$	$\bar{d}_{y,c,1} - k\bar{L}_b$
$t = hr$	$\bar{d}_{n,c,1} - k\bar{L}_h \cos v$	$\bar{d}_{x,c,1} - k\bar{L}_h$	$0.5(1 - 2\lambda)$
$t = hl$	$\bar{d}_{n,c,2} - k\bar{L}_h \cos v$	$\bar{d}_{x,c,1} - k\bar{L}_h$	$-0.5(1 - 2\lambda)$

5.3 Contribution of structural steel

The contribution of steel is calculated using basic surface integrals. In this method, the steel section is described by 16 nodes and is divided by a line parallel to the neutral axis that passes through a node (Fig. 8(a)). In this way, the steel section is divided into n curvilinear trapezoids where the top and bottom edges are lines parallel to the neutral axis, although the left and right edges can be either a straight line or a circular arc. This procedure is repeated for each value of angle v. The basic surface integral of trapezoid j is described in the $x_n y_n$ coordinate system by

$$I_{q,m}^{j} = \int\int_{trapezoid\ j} (x_n^q y_n^m) dx_n dy_n \tag{34}$$

where q and m are specific integers.

Charalampakis and Koumousis (2008) described the 16-node steel section that includes the roots (connecting flange to web). To simplify and decrease the computation cost, the roots of the steel are ignored and the section is described by 12 nodes (Fig. 8(b)). Consequently, all trapezoids have straight linear edges; otherwise, the trapezoids may consist of convex or concave edges, which make the integrals more complex. As shown in Fig. 8(b), nodal coordinates are initially expressed in an xy Cartesian system, and then transformed into a rotated $x_n y_n$ Cartesian system using Eq. (17). Table 3 shows the normalized coordinate of nodes in the xy system.

Table 3 Normalized coordinate of nodes in steel section

Node	1	2	3	4	5	6	7	8	9	10	11	12
$\bar{x}$	$\frac{W}{2}$	$-\frac{W}{2}$	$-\frac{W}{2}$	$-\frac{S}{2}$	$-\frac{S}{2}$	$-\frac{W}{2}$	$-\frac{W}{2}$	$\frac{W}{2}$	$\frac{W}{2}$	$\frac{S}{2}$	$\frac{S}{2}$	$\frac{W}{2}$
$\bar{y}$	$\frac{D+2T}{2}$	$\frac{D+2T}{2}$	$\frac{D}{2}$	$\frac{D}{2}$	$-\frac{D}{2}$	$-\frac{D}{2}$	$-\frac{D+2T}{2}$	$-\frac{D+2T}{2}$	$-\frac{D}{2}$	$-\frac{D}{2}$	$\frac{D}{2}$	$\frac{D}{2}$

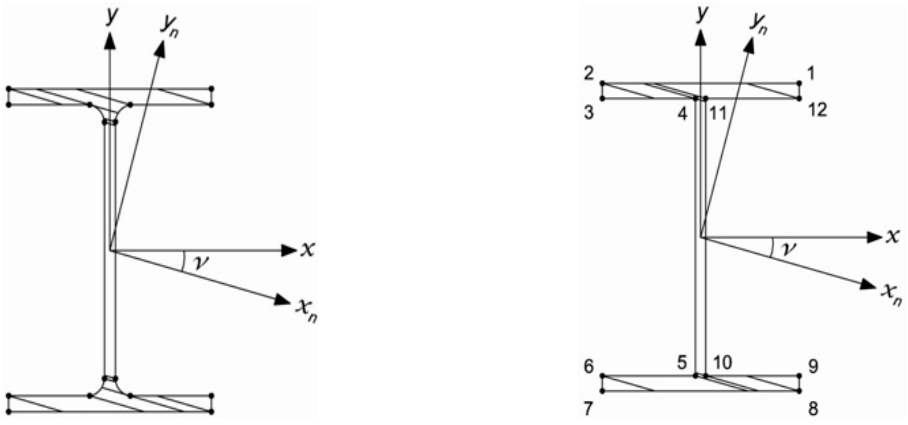

(a) 16 nodes (b) 12 nodes

Fig. 8 Decomposition of steel section into curvilinear trapezoids

Eq. (21) can be used for each segment of the stress-strain diagram (Fig. 9) for a trapezoid in a specific segment of the steel stress-strain diagram. For example, a cubic segment is formed by four points and a linear segment by two points. If a trapezoid includes a transition between segments of the stress-strain diagram, it is divided into two by a line parallel to the neutral axis. Consequently, all trapezoids are covered by a single segment. Integration of the stress field over the area of the trapezoids develops the normalized axial load and moments of each trapezoid along the x_n and y_n axes

$$n_s^j = \frac{N_s^j}{bhf_c'} = \iint_{trapezoid\ j}\left(\sum_{i=0}^{3} b_i.\bar{y}_n^i\right)dA = \sum_{i=0}^{3} b_i.\iint_{trapezoid\ j}(\bar{y}_n^i)dA = \sum_{i=0}^{3}(b_i.I_{(0,i)}^j) \tag{35a}$$

$$\begin{aligned} m_{us,x_n}^j &= \frac{M_{us,x_n}^j}{b^2hf_c'} = \iint_{trapezoid\ j}\left(\sum_{i=0}^{3}(b_i.\bar{y}_n^i)\bar{y}_n\right)dA \\ &= \sum_{i=0}^{3}\left(b_i.\iint_{trapezoid\ j}(\bar{y}_n^{i+1})dA\right) = \sum_{i=0}^{3}(b_i.I_{(0,i+1)}^j) \end{aligned} \tag{35b}$$

$$\begin{aligned} m_{us,y_n}^j &= \frac{M_{us,y_n}^j}{b^2hf_c'} = \iint_{trapezoid\ j}\left(\sum_{i=0}^{3}(b_i.\bar{y}_n^i)\bar{x}_n\right)dA \\ &= \sum_{i=0}^{3}\left(b_i.\iint_{trapezoid\ j}(\bar{y}_n^i.\bar{y}_n)\bar{x}_n dA\right) = \sum_{i=0}^{3}(b_i.I_{(1,i)}^j) \end{aligned} \tag{35c}$$

The expressions $I_{(0,i)}^j, I_{(0,i+1)}^j$ and $I_{(1,i)}^j$ are described in Appendix. By summing the stress resultants of all trapezoids, the overall axial load and bending moments are

$$n_s = \sum_{j=1}^{n} n_s^j \tag{36a}$$

$$m_{us,x_n} = \sum_{j=1}^{n} m_{us,x_n}^j \qquad m_{us,y_n} = \sum_{j=1}^{n} m_{us,y_n}^j \tag{36b}$$

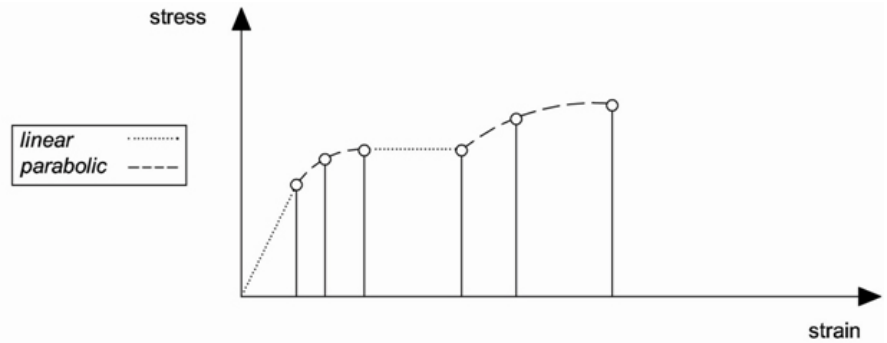

Fig. 9 Stress-strain diagram of steel

Eq. (36a) is the total normalized axial load of the steel section. The ultimate moments along the x and y axes are obtained by the inverse rotational transformation of Eq. (17)

$$\begin{bmatrix} m_{ms,x} \\ m_{us,y} \end{bmatrix} = \begin{pmatrix} \cos v & \sin v \\ -\sin v & \cos v \end{pmatrix} \begin{bmatrix} m_{us,x_n} \\ m_{us,y_n} \end{bmatrix} \tag{37}$$

6. Section geometry and reinforcement of RC circular section

The circular section has diameter D. The distribution of the longitudinal reinforcement bars is symmetric to the principal axes and comprises n_R bars of the same diameter and a total area A_r. The distance between the centroid of the reinforcement bars and the closest concrete surface is defined by c. In this section, all lengths and distances are normalized with respect to D. The dimensionless parameter corresponding to the distribution of reinforcement is

$$\omega_r = \frac{A_r}{A_c}\frac{f_{yr}}{f_c'} = \frac{A_r}{\pi D^2/4}\frac{f_{yr}}{f_c'} \tag{38}$$

where A_c is the area of the concrete core. The ratio of reinforcement in the cross-section is expressed by

$$\rho_r = \omega_r \frac{f_c'}{f_{yr}} \tag{39}$$

and the dimensionless parameter denoting the section geometry is

$$\lambda = \frac{c}{D} \tag{40}$$

7. Limit state of circular section

Fig. 10 shows a limit state for a circular section under axial loading and biaxial bending. The value of x_c is normalized with respect to D

$$\bar{x}_c = \frac{x_c}{D} \tag{41}$$

and the normalized curvature is

$$\tilde{\varphi}_u = \frac{\varphi_u D}{\varepsilon_{co}} = \frac{\varepsilon_{cu}}{\varepsilon_{co}}\frac{D}{x_c} = \frac{\mu_c}{\bar{x}_c} \tag{42}$$

The stress-strain relation of materials is the same as for Section 4; thus, the normalized axial load and components of moment are expressed as

$$n = \frac{N}{D^2 f_c'} \quad m_{ux} = \frac{M_{ux}}{D^3 f_c'} \quad m_{uy} = \frac{M_{uy}}{D^3 f_c'} \tag{43}$$

8. Contribution of materials to the bearing capacity of circular section

8.1 Contribution of concrete core

The division and numbering of the strips are shown in Fig. 11. The dimensionless parameters of the strips are described as

$$\bar{h} = \frac{x_c}{N_{st}} \quad \bar{e}_k = (k - 0.5)\bar{h} \quad \bar{l}_k = 2(\bar{e}_k - \bar{e}_k^2)^{\frac{1}{2}} \tag{44}$$

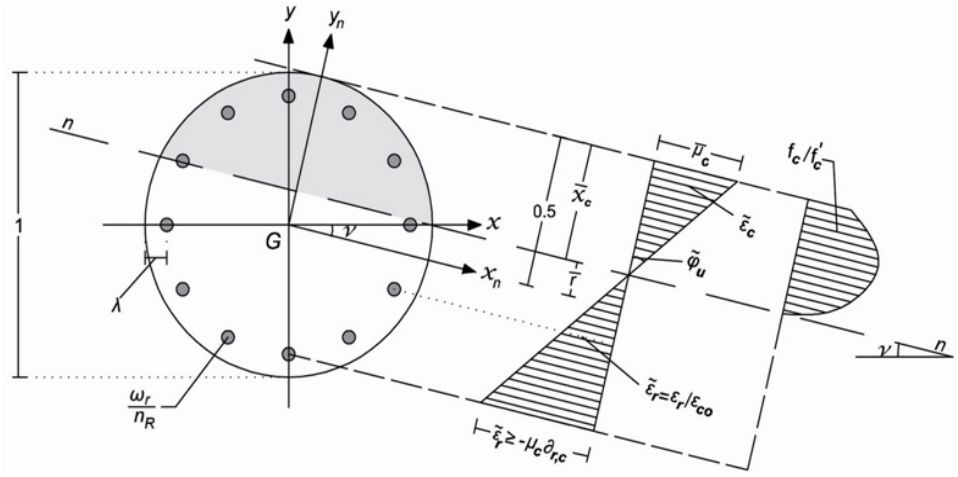

Fig. 10 Ultimate state of RC circular section under axial loading and biaxial bending

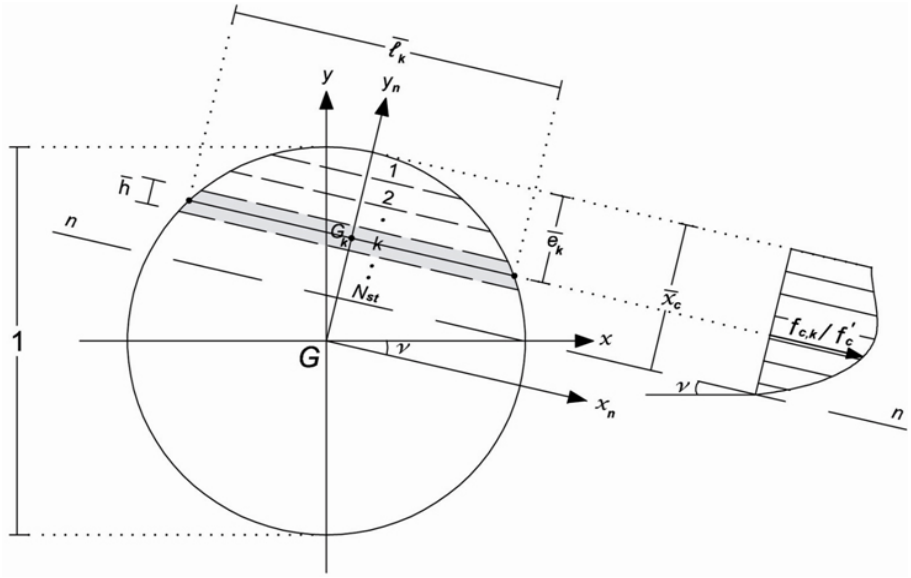

Fig. 11 Strip model of compressed concrete region in circular section

and the normalized distances of the strips from the n, x and y axes are shown in Table 4. The contribution of the concrete is described as

$$n_c = \frac{N_c}{D^2 f_c'} = \overline{h} \sum_{k=1}^{N_{st}} \overline{l}_k \frac{f_{c,k}}{f_c'}$$
$$m_{uc,j} = \frac{M_{uc,j}}{D^3 f_c'} = \overline{h} \sum_{k=1}^{N_{st}} \overline{l}_k . \overline{d}_{j,k} \frac{f_{c,k}}{f_c'}; \quad (j = x, y) \tag{45}$$

Table 4 Normalized distances of kth strip from the n, x and y axes in compressed concrete

Strip	$\overline{d}_{n,k}$	$\overline{d}_{x,k}$	$\overline{d}_{y,k}$
k	$\overline{x}_c - k\overline{h}$	$(0.5 - \overline{e}_k)\cos v$	$(0.5 - \overline{e}_k)\sin v$

8.2 Contribution of reinforcement

Fig. 12 shows the numbering of the bars. Bars placed on the x and y axes are classified as type p. Other bars are described in four zones as types a to d. Table 5 shows the normalized distances of the type p bars and Table 6 shows the normalized distances of the other types. The normalized distance between the neutral axis and the x_n axes is described by

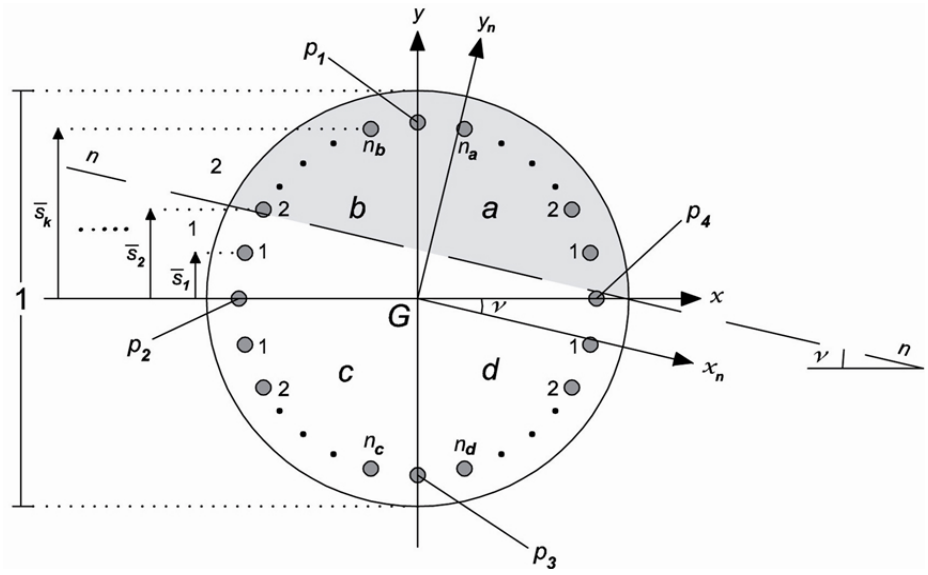

Fig. 12 Type and numbering of reinforcement bars in circular section

Table 5 Normalized distances of bars for type *p* from the *x* and *y* axes

Type of reinforcement	$\bar{d}_{x,p,k}$	$\bar{d}_{y,p,k}$
p_1	$0.5-\lambda$	0
p_2	0	$-(0.5-\lambda)$
p_3	$-(0.5-\lambda)$	0
p_4	0	$0.5-\lambda$

Table 6 Normalized distances of *k*th bar for types *a* to *d* from the *x* and *y* axes

Type of reinforcement	$\bar{d}_{x,p,k}$	$\bar{d}_{y,p,k}$
a	$\bar{s}_k$	$\bar{s}_{(n_a-k+1)}$
b	$\bar{s}_k$	$-\bar{s}_{(n_b-k+1)}$
c	$-\bar{s}_k$	$-\bar{s}_{(n_c-k+1)}$
d	$-\bar{s}_k$	$\bar{s}_{(n_d-k+1)}$

$$\bar{r}=0.5-\bar{x}_c \tag{46}$$

The coordinates of the bars are transformed by Eq. (17) into an $x_n y_n$ system. Note that the x coordinate of the bars is $\bar{d}_{y,t,k}$ and the y coordinate is $\bar{d}_{x,t,k}$. The normalized distances of the bars from the neutral axis are expressed as

$$\bar{d}_{n,t,k}=\bar{d}_{x_n,t,k}-\bar{r} \tag{47}$$

where $\bar{d}_{x_n,t,k}$ is the y_n coordinate of the *k*th type *t* bar. The contribution of the reinforcement bars is

$$\begin{aligned} n_r &= \frac{N_r}{D^2 f_c'}=\omega_r\cdot\sum_{k=1}^{n_R}\frac{\sigma_{r,t,k}}{f_{yr}} \\ m_{ur,j} &= \frac{M_{ur,j}}{D^3 f_c'}=\omega_r\cdot\sum_{k=1}^{n_R}\frac{\sigma_{r,t,k}}{f_{yr}}\bar{d}_{j,k}; \end{aligned} \qquad (j=x,y) \tag{48}$$

If the RC circular section includes an encased structural steel section, the ultimate bearing capacity of the contribution of the steel section is calculated as in Section 5.3.

9. Analysis

It is now possible to construct the $m_{uy}-m_{ux}$ and $\tilde{\varphi}_{uy}-\tilde{\varphi}_{ux}$ curves for specific values of n and v. The numerical procedure comprises three levels:

(1) The range of $0 \le v \le \pi/2$ is divided into the appropriate number of angles v so each value of v provides one point of the $m_{uy} - m_{ux}$ and $\widetilde{\varphi}_{uy} - \widetilde{\varphi}_{ux}$ curves
(2) For each value of v, the value of $\bar{x}_c$ is obtained by imposing equilibrium between assigned force (n) and ultimate load (n_u), i.e., $n = n_u$
(3) When the value of $\bar{x}_c$ is determined, the other parameters can be obtained and it is possible to calculate m_{ux}, m_{uy}, $\widetilde{\varphi}_{ux}$ and $\widetilde{\varphi}_{uy}$

For item (2) in the preceding list, increasing the value of $\bar{x}_c$ increases n_u. Therefore, for the first iteration, a very low value of $\bar{x}_c$ can be considered; for example λ (sin$v$ + cos$v$) (Fig. 7) for the rectangular section and λ for the circular section. The value of n_u is obtained by summing Eqs. (28a)-(33a)-(36a)

$$n_u = n_c + n_r + n_s \tag{49}$$

The normalized ultimate moments in item (3) are

$$m_{ux} = m_{uc,x} + m_{ur,x} + m_{us,x}, \qquad m_{uy} = m_{uc,y} + m_{ur,y} + m_{us,y} \tag{50}$$

which are the results of summing Eqs. (28b)-(33b)-(37). The components of the dimensionless curvature are

$$\widetilde{\varphi}_{ux} = \frac{\mu_c \cos v}{\bar{x}_c}, \qquad \widetilde{\varphi}_{uy} = \frac{\mu_c \sin v}{\bar{x}_c} \tag{51}$$

As in Section 3, the analysis assumes the limit state of a section and the ultimate strain of the compressed concrete at the farthest fiber from the neutral axis reaches ε_{cu}. Nevertheless, if rupture of the reinforcement at the farthest tensile fiber occurs when the maximum strain value of the compressed concrete is lower than ε_{cu}, the procedure should be revised as follows:

- For a specific value of angle v, corner bar 3 in Fig. 7 (rectangular section) is subjected to maximum tensile strain ε_{ru} with the normalized value

$$\bar{\varepsilon}_r = -\mu_r \partial_{r,c} \tag{52}$$

- For each value of $\bar{x}_c$, the normalized curvature is

$$\widetilde{\varphi}_u = \frac{\mu_r . \partial_{r,c}}{\bar{d}_{n,c,3}} \tag{53}$$

where $\bar{d}_{n,c,3}$ is the normalized (negative) distance of corner bar 3 from the neutral axis.

- The maximum strain for the compressed concrete is lower than μ_c and equals

$$\bar{\varepsilon}_{c,\max} = \widetilde{\varphi}_u \bar{x}_c \tag{54}$$

All previous expressions are modified by substituting $\bar{\varepsilon}_{c,\max}$ for μ_c.

This modification is for a rectangular section. For a circular section, the procedure is revised for the type p_3 reinforcing bar in Fig. 12. Thus, $\bar{d}_{n,c,3}$ in Eq. (53) is substituted for $\bar{d}_{n,p,3}$ to obtain the normalized curvature.

10. Validation and effectiveness of proposed formulation

To provide validation and effectiveness of the proposed method, a concrete encased steel column analyzed by Chen and Lin (2006), namely SRC2, is considered as shown in Fig. 13(a). To demonstrate the effectiveness of the normalized formulation, another cross-section with the same normalized parameters is adopted as shown in Fig. 13(b). Considering the concrete core described by the centroid line of the transverse reinforcement, the following normalized parameters are obtained for the cross-section in Fig. 13(a): $b = h = 280-2(18+4) = 236$ mm, hence: $\xi = h/b = 1$ and $\lambda = c/b = (4+8)/236 = 0.05$. The contribution of longitudinal reinforcement bars is considered symmetric which is fairy equal to the original cross-section analyzed by Chen and Lin (2006). Consequently: $\bar{L}_b = \bar{L}_h = (1-2\times0.051)/3 = 0.299$, where $n_b = n_h = 2$. For H-shape steel section: $W = 150/236 = 0.636$, $D = 130/236 = 0.551$, $T = 10/236 = 0.042$ and $S = 7/236 = 0.030$.

The value of f'_c is 28.1 MPa for unconfined concrete. By assuming the factor 1.24 for confined concrete for SRC2, f'_c is obtained 34.8 MPa. The values of f_{yr} and f_{ys} are considered equal to 350 MPa and 296 MPa, respectively. For simplicity, the stress-strain relationship of H-shape steel section is considered linear up to the yielding point, and a direct line for post-peak branch. The longitudinal reinforcement ratios with $\phi_l = 16$ mm are $A_{rc}/bh = 0.014$ and $A_{rc}/bh = A_{rh}/bh = 0.007$. Accordingly, $\omega_{rc} = 0.144$ and $\omega_{rb} = \omega_{rh} = 0.072$.

For the cross-section in Fig. 13(b), the normalized geometric parameters are: $b = h = 250 - 2(19 + 3) = 206$ mm, $\xi = 1$, $\lambda = (3 + 7) / 206 = 0.048$ and $\bar{L}_b = \bar{L}_h = (1-2\times0.048)/3 = 0.301$. The values of W, D, T and S are approximately equal to those for cross-section in Fig. 13(a). The longitudinal reinforcement ratios according to $\phi_l = 14$ mm are $A_{rc}/bh = 0.014$ and $A_{rb}/bh = A_{rh}/bh = 0.007$, therefore, the values of ω_{rc}, ω_{rb} and ω_{rh} are equal to those of the cross-section in Fig. 13(a). If the latter turn out not to be equal, the values of f'_c and f_{yr} can be considered different from those of cross-section in Fig. 13(a) to obtain a same normalized geometric and mechanical parameters. The only difference between two cross-sections is the value of parameter λ which can be considered as a mean value equal to $\lambda = 0.050$. Hence, both cross-sections can be considered to belong to the same class of composite sections with the equal expected values for dimensionless ultimate curvature and bending moment.

Assuming that the transverse reinforcement has a good effect on the confinement, The following values for the stress-strain relationship of concrete (Eq. (13)) are considered: $\alpha = 0.7$, $\eta_c = -0.1$, $\mu_c = 3.0$ and those for reinforcement (Eq. (14)) are considered: $\eta_h = 0.01$ and $\mu_r = 20$. By adopting the values of 1/200 and 0.45 for $\bar{h}$ and $\partial_{r,c}$, respectively, the interaction curves for various axial loads using the proposed formulation can be obtained as shown in Fig. 14(a). The moment domains for $N = 1000$ kPa are provided by a graphical interface program called myBiaxial, which has already been presented by Charalampakis and Koumousis (2008), and the results are compared with the results of the proposed method as shown in Fig 14(b). The axial load response provided by Charalampakis and Koumousis (2008) itself, follows the experimental curve provided by Chen and Lin (2006) fairy well.

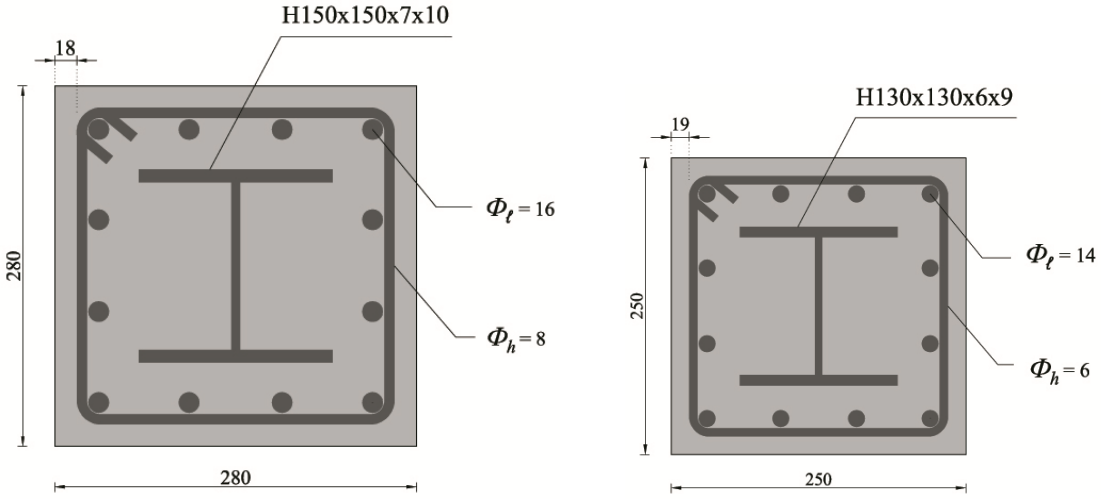

(a) Specimen 280 × 280 mm (b) Specimen 250 × 250 mm

Fig. 13 Concrete encased steel composite section (Distances in mm)

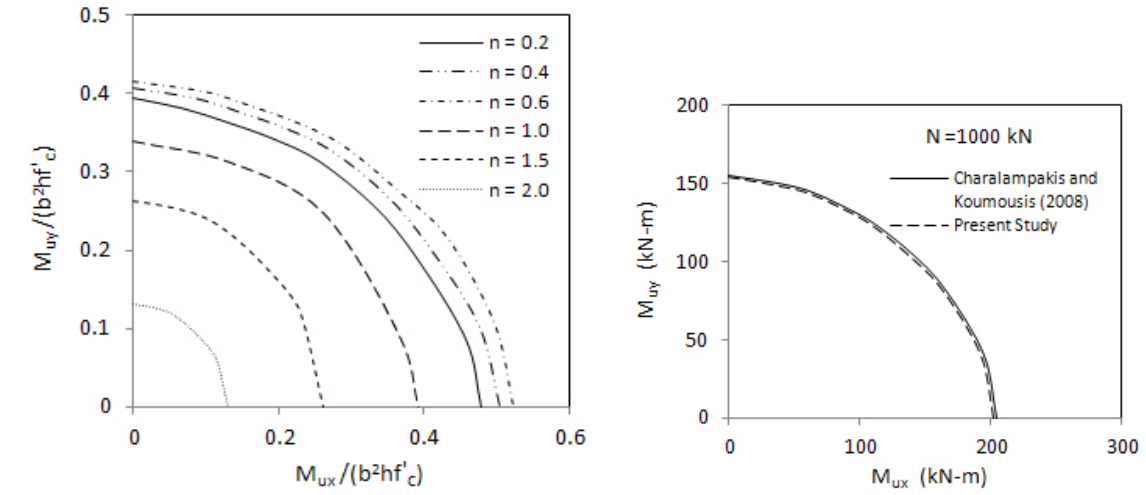

(a) Normalized interaction curves for various axial loads (b) Moment domains for N=1000 kN

Fig. 14 Interaction curves for class of concrete encased steel composite section

11. Conclusions

This study determined the ultimate curvature and moment domains for RC columns with or without an encased steel section. The cross-sections were rectangular or circular with symmetrically longitudinal reinforcement bars under biaxial loading. The study showed that the dimensionless formulation decreased the amount of computation required by the computer analysis programs. In addition, one result could be used for sections with the same normalized

parameters. An exact stress-strain relationship was used for the contribution of the materials to improve the accuracy of analysis; this allowed the use of nonlinear static and nonlinear dynamic analysis. This approach decreased the difficulty of nonlinear biaxial bending analysis by adopting an iterative procedure and defining the exact polynomial expressions for the stress-strain relationship of the steel and concrete.

References

ACI 318 (2008), Building Code Requirements for Structural Concrete and Commentary; American Concrete Institute (ACI).

Bonet, J.L., Romero, M.L., Miguel, P.F. and Fernandez, M.A. (2004), "A fast stress integration algorithm for reinforced concrete sections with axial loads and biaxial bending", *J. Comput. Struct.*, **82**, 213-225.

Bonet, J.L., Barros, M.H.F.M. and Romero, M.L. (2006), "Comparative study of analytical and numerical algorithms for designing reinforced concrete sections under biaxial bending", *J. Comput. Struct.*, **84**, 2184-2193.

Campione, G., Fossetti, M. and Papia, M. (2010), "Behavior of fiber-reinforced concrete columns under axially and eccentrically compressive loads", *Struct. J.*, **107**(3), 272-281.

Chang, G. and Mander, J. (1994), "Seismic energy based fatigue damage analysis of bridge columns: part I – evaluation of seismic capacity", NCEER Technical Rep. 94/0006; University of Buffalo, New York, NY, USA.

Charalampakis, A.E. and Koumousis, V.K. (2008), "Ultimate strength analysis of composite sections under biaxial bending and axial load", *J. Adv. Eng. Soft.*, **39**(11), 923-936.

Chen, C.C. and Lin, N.J. (2006), "Analytical model for predicting axial capacity and behaviour of concrete encased steel composite stub columns", *J. Const. Steel Res.*, **62**(5), 424-433.

Chen, S.F., Teng G. and Chan, S.L. (2001), "Design of biaxially loaded short composite columns of arbitrary cross section", *J. Struct. Eng.*, **127**(6), 678-685.

Eurocode 2 (2005), Design of Concrete Structures, Part 1-1: General rules and rules for buildings; European Committee for Standardization (CEN).

Fossetti, M. and Papia, M. (2012), "Dimensionless analysis of RC rectangular sections under axial load and biaxial bending", *J. Eng. Struct.*, **44**, 34-45.

Mander, J.B., Priestley, M.J. and Park, N.R. (1988), "Theoretical stress–strain model for confined concrete", *J. Struct. Eng.*, **114**(8), 1804-1826.

Rodriguez, J.A. and Aristizabal-Ochoa, J.D. (1999), "Biaxial interaction diagrams for short RC columns of any cross section", *J. Struct. Eng.*, **125**(6), 672-683.

Rotter, J.M. (1985), "Rapid exact inelastic biaxial bending analysis", *J. Struct. Eng.*, **111**(12), 2659-2674.

Saatcioglu, M. and Razvi, S.R. (1992), "Strength and ductility of confined concrete", *J. Struct. Eng.*, **118**(6), 1590-1607.

Saatcioglu, M., Salamat, A.H. and Razvi, S.R. (1995), "Confined columns under eccentric loading", *J. Struct. Eng.*, **121**(11), 1547-1555.

Sargin, M. (1971), "Stress-strain relationship for concrete and the analysis of structural concrete sections", Study Report 4, University of Waterloo, Ontario.

Sousa, J.B.M. and Muniz, C.F.D.G. (2007), "Analytical integration of cross section properties for numerical analysis of reinforced concrete, steel and composite frames", *J. Eng. Struct.*, **29**(4), 618-625.

Vallenas, J., Bertero, V.V. and Popov, E.P. (1977), "Concrete confined by rectangular hoops and subjected to axial loads", UCB/EERC Rep. 77/13; Earthquake Engineering Research Center, University of California, Berkeley, CA, USA.

CC

Appendix: Basic surface integrals

As shown in Fig. 13, expressions L_{14} and L_{23} are described as

$$L_{14} = \frac{(x_4 - x_1)}{(y_{34} - y_{12})} \;\&\; L_{23} = \frac{(x_3 - x_2)}{(y_{34} - y_{12})}; \quad y_{34} > y_{12}$$

Thus, the basic surface integral of trapezoid j is

$$I^j_{q,m} = \int_{y_{12}}^{y_{34}} \left(\int_{x_1 + L_{14}(y - y_{12})}^{x_2 + L_{23}(y - y_{12})} (x^q . y^m) dx \right) dy$$

Consequently

$$I^j_{(0,m)} = \frac{1}{m+2}(L_{23} - L_{14})(y_{34}^{m+2} - y_{12}^{m+2}) + \frac{1}{n+1}(x_2 - L_{23}.y_{12} - x_1 - L_{14}.y_{12})(y_{34}^{m-1} - y_{12}^{m+1})$$

$$A = \frac{1}{2}(L_{23}^2 - L_{14}^2),$$

$$B = (x_2 - L_{23}.y_{12}).L_{23} - (x_1 - L_{14}.y_{12}).L_{14},$$

$$C = \frac{1}{2}\left((x_2 - L_{23}.y_{12})^2 - (x_1 - L_{14}.y_{12})^2\right),$$

$$I^j_{(1,m)} = \frac{1}{m+3}.A.(y_{34}^{m+3} - y_{12}^{m+3}) + \frac{1}{n+2}.B.(y_{34}^{m+2} - y_{12}^{m+2}) + \frac{1}{n+1}.C.(y_{34}^{m+1} - y_{12}^{m+1})$$

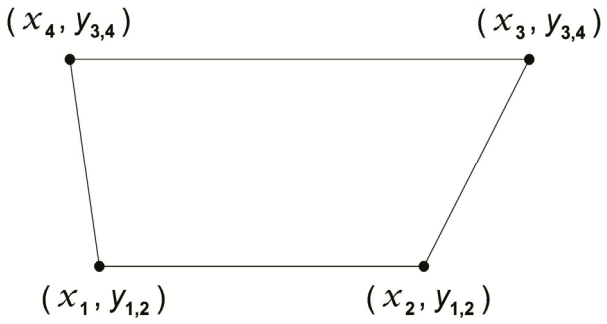

Fig. 15 Trapezoid